TESTING OF CENTRAL PIT FORMATION MECHANISMS USING INFERENTIAL STATISTICS. S. E. Peel[1] and D. M. Burr[1], [1]University of Tennessee, Knoxville, Tennessee, USA (speel1@vols.utk.edu).

Introduction: Central pit craters (CPCs) are complex craters that contain centrally located, approximately circular depressions on crater floors (floor pits) and on central peaks (summit pits), and are formed during crater emplacement [Fig. 1; e.g., 1-3]. These craters have been found on numerous bodies across the solar system [e.g., 3-9]. Because of the range of condition that apparently allow for central pit formation (ie. different target properties and gravity), the formation of central pits is not well understood.

Previously proposed formation mechanisms (Table 1) on Mars and elsewhere have been investigated using methods such as crater inventories and descriptive statistics, morphological analyses, and modeling [e.g., 10, 3, 11-13]. This work tests the formation mechanisms for Mars central pits using inferential statistical analyses based on relationships that should be present for each formation mechanism (Table 2). Because floor central pits and summit central pits may be formed by different mechanisms, the analyses for each were conducted separately.

Hypothesis	Sources
(A) Explosive release of volatiles from the subsurface	[14-17]
(B) Collapse of a central peak	[18-20]
(C) Subsurface drainage of water melt	[21]

Table 1: Previously proposed hypotheses tested in this investigation.

Hyp	(Test ID) Relationship
(A, C)	(1) CPCs should have a higher occurrence of volatile-rich ejecta than non-CPCs. [22]
(A)	(2) The volume of the central pits should be greater than the volume of their rims. [23]
(B)	(3) The diameters of central pit rims should be wider than the diameters of central peaks. [23]

Table 2: The relationships that have been proposed to support one or more of the proposed hypotheses.

Data Collection: To identify craters for this analysis, we inspected a global database of impact crater [22] to independently assess the previous identifications of central peak, floor central pit and summit central pit complex craters. Each of these complex craters was investigated to determine if it had sufficient preservation, and limited infilling, to be appropriate for each of the tests. All of these steps were conducted using CTX imagery [25] in Google Earth [26] and JMars [27] programs. Heavily modified and elongated craters were excluded from this investigation to avoid our measurements being affected by processes unrelated to central pit formation. Identifications of ejecta morphology were accomplished using CTX and THEMIS imagery.

All analyses were conducted in ArcMap [28] using sinusoidal projection. CTX digital elevation models (DEMs) were created using NASA's Ames Stereo Pipeline [29] for volume measurements and diameter measurements when necessary.

Statistical Tests: *Test 1: Occurrence of volatile-rich ejecta.* The statistical test for this analysis is the chi-square test for homogeneity, which compares the observed frequencies of one variable identity in two populations to its expected frequency. The null and alternate hypotheses for this statistical test are (H_o) *the total occurrence of volatile-rich ejecta for CPCs ≤ the total occurrence volatile-rich ejecta for non-CPC complex craters* and (H_{alt}) *the total occurrence of volatile-rich ejecta for CPCs > the total occurrence of volatile-rich ejecta for non-CPC complex craters*.

Test 2: Feature volume. The statistical test for this analysis is the t-test for two dependent samples, which tests if the values of two dependent variables are equal. The null and alternate hypotheses for this statistical test are (H_o) *mean volume of the pit rim ≥ mean volume of the pit* and (H_{alt}) *mean volume of the pit rim < mean volume of the pit*. After plotting topographic contours from the CTX DEMs for each crater, we derived volumes by identifying the elevation of the vertical contact between the central pit and pit rim, converting that contour into a plane, and extracting the volumes of the features bounded by this plane and the DEM surface (Fig. 2). The volume of the pit is the volume below the plane that is contained within the DEM surface and the plane. The volume of the rim is the volume above the plane that is contained within the DEM surface and the plane.

Test 3: Feature diameter. The statistical test for this analysis is the t-test for two independent samples, which tests if the values of two independent variables are equal. The null and alternate hypotheses for this statistical test are (H_o) *mean central pit rim diameter ≤ mean central peak diameter* and (H_{alt}) *mean central pit diameter rim > mean central peak diameter*. Central pit and central peak diameter measurements were conducted in ArcMap. The diameters are determined using an

enclosing circle. The central pits are measured from the outermost extent of the highest surroundings (ie. rim) on one side to the opposite side of the feature. The diameters of the central peaks are measured from the farthest extent of the central peak structure on one side to its opposite side. The diameter measurements for both features are normalized to the host crater diameter.

Statistical Power Analyses: The selected maximum probability of committing a type 1 error (α), rejecting a null hypothesis that is true [30-33], for this investigation is 0.05. The selected maximum probability of committing a type 2 error (β), accepting a null hypothesis that is false [30-33], for this investigation is 0.2. Power (*P*, where *P*=1-β) is the likelihood that the test will correctly reject a false null hypothesis [30-32], and is 0.8. Because there are three statistical tests being conducted, the values of α, β, and *P* for each of the tests must sum to the values selected for the total investigation [32, p. 688]. For this investigation, each of the tests is conducted at or below α=0.017, β=0.067, and *P*=0.933 [32-34].

Power analyses were conducted in RStudio [35] using the *pwr* package [36] to determine the necessary sample sizes (n) for each of the statistical tests given the selected values of α=0.017, β=0.067, *P*=0.933, and minimum effect size (ES) that can be detected (difference from statistical null hypothesis, [32, 34]). For Test 1, n=168 for ES=0.3. For Test 2, n=85 for ES=0.4. For Test 3, n=165 for ES=0.4.

References: [1] Smith, E. I. (1976) *Icarus 28*, 543-550. [2] Hale, W. S., Head, J. W. (1981) *LPI Contr. 441*, 104-106. [3] Barlow, N. G. (2010) *GSA Special Papers 465*, 15-27. [4] Croft, S. K. (1983) *JGR: Solid Earth (1978-2012) 88.S01:* B71-B89. [5] Moore, J. M., Malin, M. C. (1988) *GRL 15*, 3, 225-228. [6] Schenk, P. M. (1993) *JGR 98*, E4, 7475-7498. [7] Xiao, Z., Komatsu, G. (2013) *Planet. and Space Sci. 82-83*, 62-78. [8] Xiao, Z., Zeng, Z., Komatsu, G. (2014) *Icarus 227*, 195-201. [9] Russell, C. T. (2015) *DPS 47*, abs. #201.01. [10] Barlow, N. G. (2006) *Meteoritics and Planet. Sci. 41*, 1425-1436. [11] Senft, L. E., Stewart, S. T. (2011) *Icarus 214*, 67-81. [12] Elder, C. M., Bray, V. J., Melosh, H. J. (2012) *Icarus 221*, 831-843. [13] Barlow, N. G. (2015) *GSA Special Paper 518*, 1-34. [14] Hodges, C. A. (1978) *LPS 9*, 521-522. [15] Hodges, C. A. (1978) *NASA Tech. Mem. 79729*, 169-171. [16] Wood, C. A., Head, J. W., Cintala, M. J. (1978) *Proc. LPSC 9*, 3691-3709. [17] Wood, C. A., Cintala, M. J., Head, J. W. (1978) *Rep. Planet. Geol. Prog. 1977-1978*, 166-168. [18] Greeley, R. et al. (1982) *Satellites of Jupiter*, 340-378. [19] Passey, Q. R., Shoemaker, E. M. (1982) *Satellites of Jupiter*, 379-434. [20] Schenk, P. M. (1993) *JGR 98*, E4, 7475-7498. [21] Croft, S. K. (1981) *LPISC 12*, 196-198. [22] Barlow, N. G. (2009) *LPSC 40*, abs. #1915. [23] Bray, V. J., Schenk, P. M., Melosh, H. J., Morgan, J. V., Collins, G. S. (2012) *Icarus 217*, 115-129. [24] Robbins, S. J., Hynek, B. M. (2012) *JGR 117*, Res. 117, E06001, DOI: 10.1029/2011JE003967. [25] Malin, M. C. et al. (2007) *JGR: Planets (1991-2012), 112(E5)*. [26] Google Inc. (2009), v. 7.1.7.2600 [Software] www.google.com/earth/. [27] Christensen, P.R. et al. (2009) abs. #IN22A-06. [28] ESRI (2011) ArcGIS Desktop: Resease 10.1. Redlands, CA: Environmental Systems Research Institute. [29] Moratto, Z. M. et al. (2010) *Proc. LPS XLI*, abs. #2364. [30] Harnett, D. L. (1982) *Statistical Methods, 3rd Ed.* Addison-Wesley, Reading. [31] Chiang, C. L. (2003) *Statistical methdos of analysis*. World Scientific, Singapore. [32] Sheskin, D. J. (2004) *Handbook of Parametric and Nonparametric Statistical Procedures, 3rd Ed.* Chapman & Hall/CRC, Boca Raton. [33] Burt, J. E., Barber, G. M., Rigby, D. L. (2009) *Elementary Statistics for Geographers, 3rd Ed.* The Guilford Press, New York. [34] Cohen, J. (1992) *A Power Primer*. Psychological Bulletin, 155-150, v. 112. [35] RStudio Team (2015) RStudio: Integrated Development for R. RStudio, Inc., Boston, MA. www.rstudio.com. [36] Champely, S. (2016) *Pwr: Basic Functions for Power Analysis.* R package version 1.2-0.

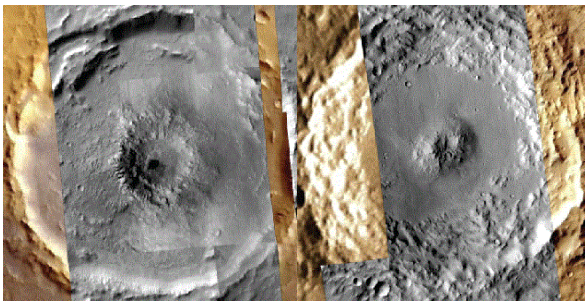

Fig. 1: CTX imagery atop Viking and Mars Global Surveyor imagery showing a (lt) floor central pit crater (-17.7N, -63.6E; diam. ~50 km; image data: Google, NASA/USGS) and (rt) summit central pit crater (2.67N, 110.4E; diam. ~44km; image data: Google, NASA/USGS/ESA/DLR/FU Berlin (G. Neukum)).

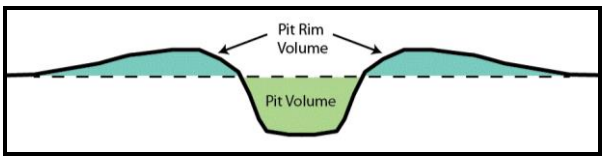

Fig. 2: Diagram showing how the volumes of the pits and pit rims are defined. The dashed line is the plane defined by the elevation contour. The solid line is the DEM surface.